frontiers in Energy Research

REVIEW
published: 30 March 2022
doi: 10.3389/fenrg.2022.844729

Methods for Remit Voltage Reversal of Proton Exchange Membrane Fuel Cells

Zi'ang Xiong[1], Bo Wen[2], Dustin Banham[3], Siew Hwa Chan[4,5], Zhiyong Xie[1]*, Yili Liang[1] and Shijun Liao[6]*

[1]Powder Metallurgy Research Institute, Central South University, Changsha, China, [2]School of Materials Science and Engineering, Xiangtan University, Xiangtan, China, [3]School of Materials Science and Hydrogen Energy, Foshan University, Foshan, China, [4]School of Mechanical and Aerospace Engineering, Nanyang Technological University, Singapore, Singapore, [5]Energy Research Institute at NTU (ERI@N), Nanyang Technological University, Singapore, Singapore, [6]School of Chemistry and Chemical Engineering, South China University of Technology, Guangzhou, China

In the commercialization of the hydrogen fuel cell for the transportation sector, one of the main factors affecting the lifespan of the fuel cell is voltage reversal, especially when the anode of the fuel cell is subject to fuel starvation momentarily during the operation. In this article, mitigation methods for voltage reversal are summarized in three parts, namely, the catalyst approaches, the MEA design approaches, the stack and system strategies approaches, which include the application of a highly active oxygen evolution reaction (OER) catalyst or durable catalyst support in the anode, employing a protective layer for the catalyst layer or optimizing the formula of the catalyst layer or employing a durable GDL, or optimization of stack design or system operation strategies.

Keywords: voltage reversal, oxygen evolution reaction, carbon corrosion, water electrolysis, durability, reversal tolerance anode

Edited by:
Daniel Zanetti De Florio,
Federal University of ABC, Brazil

Reviewed by:
Chanho Pak,
Gwangju Institute of Science and Technology, South Korea
Peter Pintauro,
Vanderbilt University, United States

****Correspondence:***
Zhiyong Xie
xzy507@csu.edu.cn
Shijun Liao
chsjliao@scut.edu.cn

Specialty section:
This article was submitted to Fuel Cells,
a section of the journal
Frontiers in Energy Research

Received: *28 December 2021*
Accepted: *04 March 2022*
Published: *30 March 2022*

Citation:
Xiong Z, Wen B, Banham D, Chan SH, Xie Z, Liang Y and Liao S (2022) Methods for Remit Voltage Reversal of Proton Exchange Membrane Fuel Cells.
Front. Energy Res. 10:844729.
doi: 10.3389/fenrg.2022.844729

INTRODUCTION

In an effort to decarbonize the transportation sector, there has been a solid desire to electrify the drivetrain of both commercial and passenger vehicles. The approaches include hybrid vehicles, lithium battery vehicles, and hydrogen fuel cell vehicles. Specifically, for commercial vehicles such as buses and trucks, the fast refueling and long-distance driving range can be achieved by hydrogen fuel cells. Additionally, hydrogen fuel cells exhibit high energy density, high energy conversion efficiency, and zero on-site pollution (Peng et al., 2015; Xiong et al., 2015; Jia et al., 2017; Yanzhou, 2017; Bizon et al., 2019; Huang et al., 2020). Hyundai, Toyota, Honda, and other car companies have launched various fuel cell vehicles, and in China, this technology is being used to replace diesel engines. However, fuel cells are yet to achieve significant cost reduction to expand their commercial footprint. To lower the cost of fuel cell stacks, approaches such as utilizing non-Pt catalysts to replace the Pt/C (Peng et al., 2013; Liu et al., 2014a; You et al., 2014; Nakashima, 2019; Sibul et al., 2020) and self-humidifying membrane electrode assembly (MEA) to reduce the size/cost of the humidifier (Fan et al., 2017; Anu and Cindrella, 2019; Hou, 2019; Shin, 2020) have been investigated. To improve the performance of fuel cells, significant research has been focusing on the synthesis of catalysts (particularly the cathode) (Paul et al., 2015; Dang et al., 2017; Dustin et al., 2019; Chalgin, 2020) and extensive efforts have been carried out to understand the mechanism of degradation (Liu et al., 2014b; Jia et al., 2016; Shen, 2020; Vichard et al., 2020; Chen et al., 2021a; Hu, 2021; Rui, 2021).

During normal fuel cell operations, electrode potential drives the desired electrochemical reactions, namely, the oxygen reduction reaction (ORR) at the cathode and the hydrogen

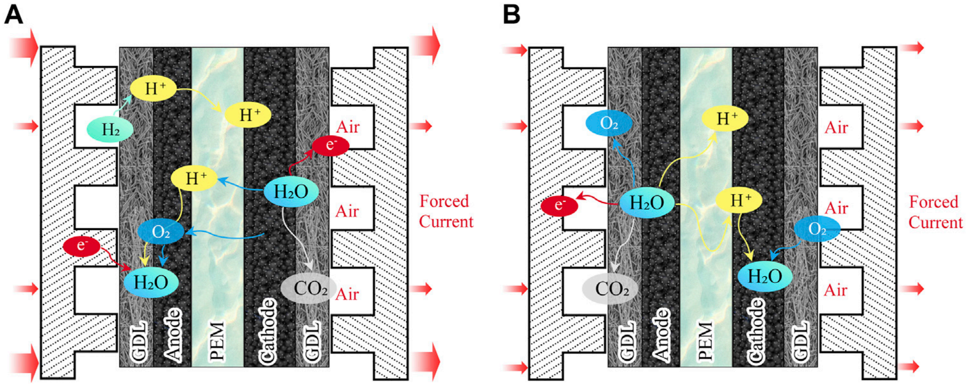

FIGURE 1 | Difference between local H_2 starvation and overall H_2 starvation.

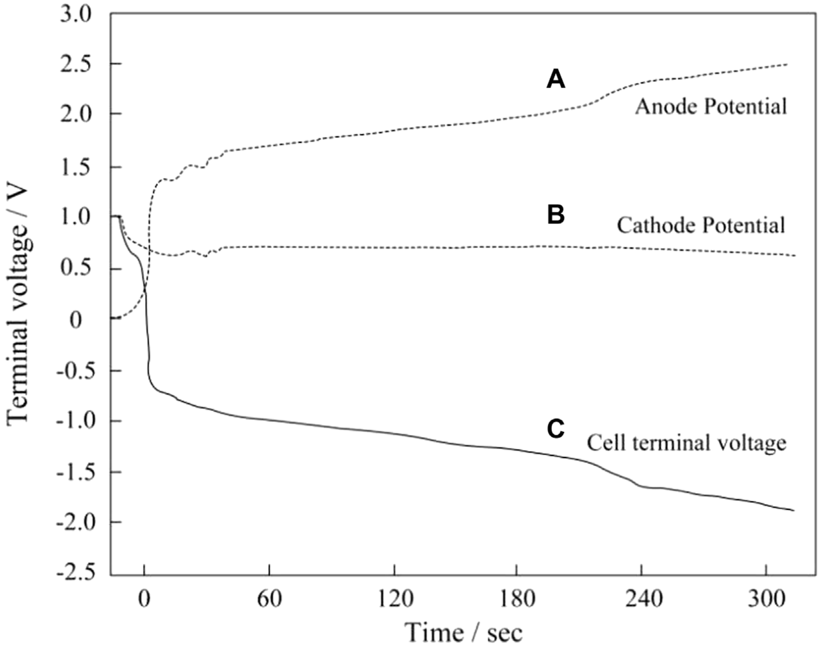

FIGURE 2 | Potential profile of the single cell during the simulated cell reversal event. Reproduced with permission (Taniguchi et al., 2004). Copyright 2004, Elsevier.

oxidation reaction (HOR) at the anode. Under normal circumstances, both the anode and the cathode have excess hydrogen and air supply, respectively. However, there are circumstances that cause drastic potential excursions at the electrode, such as low catalyst performance, insufficient supply of reactants, uneven gas distribution, rapid changes in load, and startup or shutdown operations. These failure modes are known to degrade the performance of MEA rapidly, and hence degrade the performance of the fuel cell stack as a whole (Chen et al., 2019; Wh, 2021; Jia et al., 2015; Cheng, 2015; Zhao, 2020).

For a commercial application, one of the most damaging factors is the global fuel starvation. This occurs when complete blockage of H_2 occurs at the anode of one or more MEAs, while the other MEA in the stack continues to operate normally. As shown in **Figure 1A**, local fuel starvation leads to current reversal, while overall fuel starvation leads to voltage reversal as shown in **Figure 1B**. A slight fuel shortage occurs during low stoichiometric ratio or a surge in load demand, and these may resulting in local fuel starvation. Low pressure caused by local fuel starvation would result in the permeation of air; accordingly, carbon corrosion takes place in regions facing air/H_2 boundary and in the cathode. When the stoichiometric ratio of fuel is less than 1, overall fuel starvation occurs. Once the fuel cell has been forced to sustain the current, carbon oxidation reaction (COR) and OER would take place to provide protons and electrons. When this happens, as is shown in **Figure 2**, the

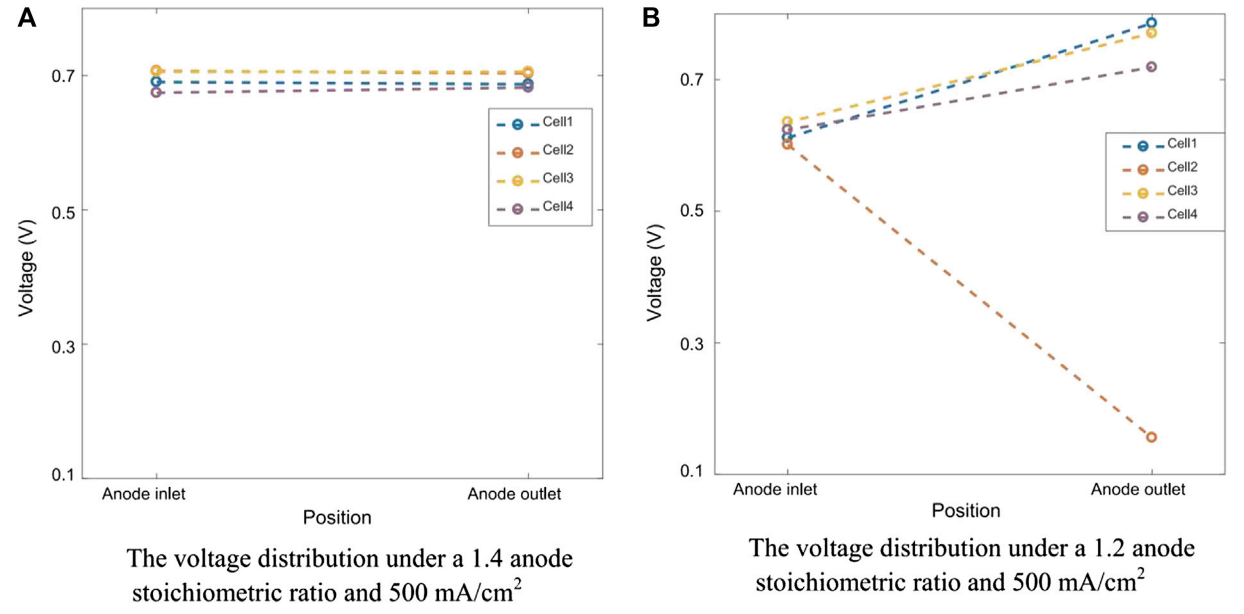

FIGURE 3 | Voltage difference between the two ends of the cells. Reproduced with permission (Hu et al., 2018). Copyright 2018, Elsevier.

anode potential of the fuel-starved MEA is driven to excessively high potentials (>2 V), leading to the rapid oxidation of the anodic carbon structure. Meanwhile, the cell voltage drops rapidly until below 0 V, and the fuel cell turns into an electrolyzer. This failure must be differentiated from local fuel starvation, which leads to a very different failure mode in which the cathodic carbon structure would be damaged. At the same time, the anode does not experience any high potential.

When hydrogen is not supplied to the anode, the voltage of the MEA decreases rapidly in a few seconds due to the raising of the anode potential. The reversal occurs when the anode potential exceeds the cathode potential. When the anode potential rises to 1.5 V, both carbon corrosion and water electrolysis occur to provide electrons and protons, rather than the normal hydrogen oxidation reaction to provide protons and electrons (Zhang et al., 2012; Yi, 2012; Dong, 2009). The result of these reversal events is carbon corrosion and sintering of Pt particles leading to significant damage to the anode catalyst layer and eventually complete failure of the MEA. Carbon corrosion of the anode near the outlet of the stack is often more severe than that of the inlet due to H_2 concentration gradients through the flow fields (Yi, 2012). As shown in **Figure 3**, the voltage of the two ends of singles cells have been compared under different fuel stoichiometry. Compared with single cells in **Figure 3A**, and the single cells in **Figure 3B** that is partially fuel starved is found to quickly suffer from voltage drop (Hu et al., 2018). Water electrolysis and carbon corrosion are concurrent. However, the anode potential determines the relative rate of the two reactions. Water electrolysis is favored at cell voltages between −0.9 V and −1.1 V (Velikokhatnyi et al., 2013; Liu et al., 2014b; Wang et al., 2020a; Wang et al., 2020b), while carbon corrosion is favored between −1.7 and 2.0 V (Hasché et al., 2010; Dhanushkodi et al., 2013; Pandy et al., 2013). Prolonging the reaction of water electrolysis is helpful to alleviate the occurrence of carbon corrosion reaction (Lee et al., 2021a).

Overcoming reversal has been a key focus within the fuel cell industry. However, it has received relatively less attention within academia. However, with the rapid growth of the PEMFC industry in recent years, and the large-scale deployment of the technology, the importance of solving this critical issue has gained momentum in the academic research community. Lots of work on reversal tolerance anode (RTA) strategy were explored; to reduce the influence of fuel starvation, RTA uses OER catalyst, which promotes the electrolysis of water and reduces the rate of COR. In this review article, approaches to solving this technical challenge are categorized and discussed according to the 1) materials level (catalyst solutions), 2) MEA level (anode/MEA design solutions), and 3) stack and system level. Following a review of recent literature, concluding remarks on future directions are made.

CATALYST APPROACHES

Previous studies suggested that COR and MEA deterioration can be suppressed by adding OER catalyst into the anode. Using oxidation-resistant carbon supports is also helpful in alleviating carbon corrosion (Petch et al., 2015). Thus, from the level of the material, approaches to overcoming reversal have focused on developing a highly active OER catalyst and a highly durable HOR catalyst.

Development of Highly Active OER Catalyst

Tita Labi (2021) prepared graphitized Vulcan carbon black-supported IrO_x catalyst (IrO_x/GV) by the microwave-assisted polyol deposition technology. The mass fraction of Ir in IrO_x/GV

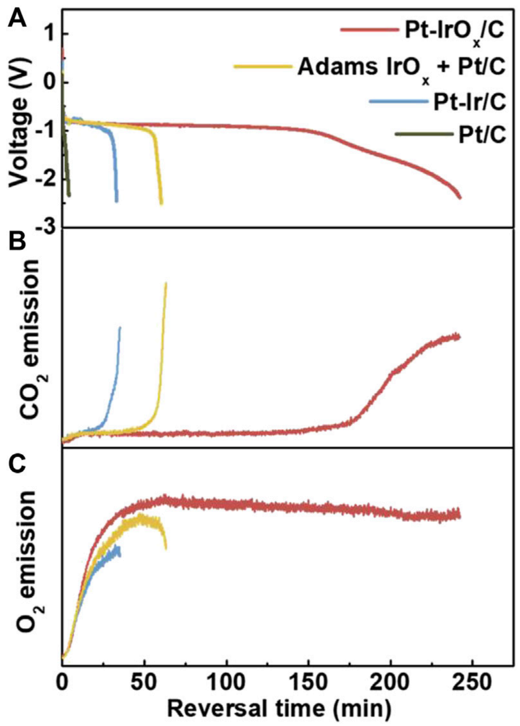

FIGURE 4 | Reversal tolerance ability of various RTAs. Release of **(B)** CO_2 (m/z 44) and **(C)** O_2 (m/z 32) during the voltage reversal test. Reproduced with permission (Roh et al., 2019). Copyright 2019, Elsevier.

is 56wt%, and the Ir nanoparticles are 4–8 nm. IrOx/GV was added to the anode CL as an OER catalyst, and the loading of Ir in the CL was 0.1 mg/cm^2. After 5 min, 10 min, and 30 min of the intermittent reversal test, the reversal voltage is basically maintained at –0.8 V; after the reversal test, the performance is kept at 95% of the initial performance of the fuel cell, without causing serious performance damage. Through SEM and EIS analysis, the attenuation of the performance was found to be mainly due to the loss and shrinkage of the proton exchange membrane (PEM) and the structural deformation of the ionomer affecting the proton transport pathway. The anode CL inevitably becomes thinner, which leads to the decline in performance and increase in contact resistance. In addition, it was found that the Pt/C is stable in the short-term intermittent starvation process, while it becomes charged and soluble in the long-term instigation reversal process.

However, due to the difference in the surface characteristics of Pt/C and IrO_2, it is still a challenge for IrO_2 to be uniformly dispersed in the catalyst slurry. At the same time, the loading of Pt/C and IrO_2 catalysts will also be reduced. Compared with directly mixing IrO_x prepared using the Adams me1lting method with commercial Pt/C as the reversal tolerance anode, Roh et al. (2019) deposited IrO_x on the surface of the commercial Pt/C catalyst. As is shown in **Figure 4**, compared with the mixture of IrO_x and commercial Pt/C, IrO_x-Pt/C can protect the carbon support from carbon corrosion, as **Figure 4A** shows, the durability is increased by four times. The OER ability of different catalyst has been verified by on-line monitoring the release rate of CO_2 and O_2 as shown in **Figures 4B,C**. At the same time, the anti-reversal effect of IrO_x and Ir were compared, and it was found that the anti-reversal effect of Ir was very poor, mainly because Ir could also participate in the competition of HOR reaction and Ir was easily poisoned by CO.

Lee et al. (2021b) synthesized graphitized carbon-supported Ir-Ru alloy as an anti-reversal OER catalyst as $IrRu_2$ alloy particles have good particle size distribution. The activity of $IrRu_2$ with grain diameter less than 5.33 nm is 1.1 times higher than the activity of Pt/C. Through the simulated reversal test, using $IrRu_2$/C as an anode catalyst, the durability was actually up to 7 h, while using only a Pt/C catalyst, the durability was only approximately 10 min. The modified IrRu alloy catalyst is expected to be used as an anode catalyst and replace Pt in PEMFC. The surface segregation of Ir in the IrRu alloy would downshift the d-band which lead to the decrease of hydrogen adsorption energy, resulting in high catalytic activity (Lile, 2021). Xiangyang Zhou et al. (Zhou et al., 2020) prepared the IrO_2/RuO_2 catalyst using the improved Adams melting method. In the half-cell, the durability of the MEA with the IrO_2/RuO_2 catalyst was improved, the activity decreased slightly, and the voltage of the single cell at 1 A/cm^2 and the maximum power density decreased by 2.8 and 8.7%, respectively. The durability was prolonged from 0.67 to 66 min, the H_2 starvation test was repeated, and the cumulative durability was as long as 78 h. You et al. (2020) reported the effects of the ratio of Ru to Ir in alloy catalysts and the graphitization extent of the carbon support on the reversal tolerance ability. The impregnation reduction method was used to prepare Ru_xIr_y alloy catalysts, and the carbon support was treated at different high temperatures. The results show that the crystalline structure of Ru_xIr_y is hexagonal with the increase in Ru content. Under the condition of single-cell test, the performance of Ru_xIr_y alloy is similar to that of the Pt/C catalyst. Moreover, the Ru_xIr_y alloy catalyst showed a coordinated lifting effect, and the reversal tolerance ability was better than that of the mixed Ir and Ru catalysts in the same proportion. With the same proportion of Ru_xIr_y alloy, the higher the graphitization degree of the carbon support, the better the antireversal ability of MEA. Kim et al. (2020) prepared Ir-Ru/C alloy catalysts using the impregnation reduction method. The effects of different reduction temperatures in a hydrogen atmosphere and different heat treatment temperatures in a nitrogen atmosphere on the OER and HOR properties of the Ir-Ru/C alloy catalysts were investigated. The results showed that the precursors of Ir and Ru can also be reduced in a nitrogen atmosphere. The $IrRu_4$/C reduced at 200°C in the hydrogen atmosphere shows better electrochemical activity and stability than $IrRu_4$/C prepared at 300°C, which is related to the low crystallization on the surface of catalyst particles under mild heat treatment. The properties of $IrRu_4$/C at different heat treatment temperatures in the nitrogen atmosphere are the same as those of $IrRu_4$/C prepared in the hydrogen atmosphere. However, the performance of $IrRu_4$/C prepared at 900°C in the nitrogen atmosphere is similar to that of $IrRu_4$/C prepared in the hydrogen atmosphere.

Lee et al. (2019) synthesized graphitized carbon-supported $IrRu_4Y_{0.5}$ ternary alloy catalyst, which showed 21% higher performance and better antireversal durability than Pt/C. It is considered that the IrRuY-based catalyst is expected to displace the Pt-based catalyst as the bifunctional catalyst of HOR and OER. Cullen et al. (2014) reported the OER catalyst would limit the migration of dissolved Pt. This is because Ir tends to exist in the form of highly dispersed nanoparticles, while Pt tends to exist in the form of large particle agglomeration. Ir migrated into the PEM provides nuclei for Pt, which limits further migration of Pt to the PEM. Ru is easier to dissolve than Pt and Ir, but migrates to MPL rather than PEM. Moore et al. (2019) investigated the OER activity and durability of IrO_2 with different crystallization and IrO_x/TiO_2 with TiO_2 as support using the non-in situ accelerated pressure test. The results showed that the higher the crystallization of IrO_2, the longer the reversal tolerance durability, the higher the specific surface area of IrO_2, and the better the mass activity. Compared with IrO_2 without support, IrO_x/TiO_2 has the best mass activity, but the dissolution concentration of Ir is the highest, which may be due to Ti^{3+} acting as a reducing agent, leading to the dissolution of IrO_2, and the formation of oxygen vacancy in TiO_2 support is helpful in improving the OER activity of IrO_x/TiO_2. Tovini et al. (2020) confirmed the surface of IrO_2 particles will be reduced to Ir by H_2, and the Ir will dissolve, diffuse through the membrane, and be deposited on the cathode Pt/C during repeated start-up and shutdown, resulting in the decrease in the cathode ORR activity. The Ir in the cathode CL can be observed with the help of XPS. At the same time, repeated start and stop will also result in the loss of decreased OER activity because the anode Pt will be dissolved and deposited on the surface of IrO_2 to block the OER active site. The chemical stability of IrO_2 should be considered when IrO_2 is blended with Pt/C as an anode catalyst.

Development of Durable HOR Catalysts

The occurrence of carbon corrosion will not only cause an increase in electrical resistance, but also increase the hydrophilicity of carbon support which leads to flooding (Taniguchi et al., 2004). Some support shows a positive effect on the catalyst, for instance, enhanced active surface area, improved activity, long service life, etc (Puthiyapura et al., 2014; Liu et al., 2020; Bhanja et al., 2019; Min et al., 2017). Kumar et al. (2017) synthesized an anode catalyst with 40wt.% Pt on RuO_2-TiO_2. Compared with TKK TEC10EA30E, the voltage of Pt/RuO_2-TiO_2 remained stable after 400 cycles of reversal test, which was related to the corrosion resistance of the support and the excellent OER activity of RuO_2. Using Ti_4O_7 as catalyst support also has a good reversal tolerance ability. Ti_nO_{2n-1} ($4 < n < 10$) of Magneli phase has been considered for various electrochemical applications because of its chemical stability and electrical properties. The conductivity of Ti_nO_{2n-1} increases with the decrease in n, and the conductivity of Ti_4O_7 is similar to that of graphite. Tsutomu Ioroi et al. (Ioroi and Yasuda, 2020) prepared Ti_4O_7 by pulsed ultraviolet laser irradiation on TiO_2, then impregnated and reduced Pt/Ti_4O_7 catalyst, and then supported a small amount of Ir on Pt/Ti_4O_7 by impregnation reduction. The reversal tolerance performance of Pt/C, Pt/GKB, and Pt/Ti_4O_7 catalysts was compared, and it was found that the reversal tolerance performance of the Pt/Ti_4O_7 catalyst was the best. At the same time, the reversal tolerance performance of Pt/Ti_4O_7 with different loading of Ir was compared. The results showed that the reversal tolerance ability improved with the increase of Ir content. For the catalyst supported by trace Ir on Pt/Ti_4O_7, although the loading of Ir is only 0.014 mg/cm^2, the durability is still as long as 7200 s. As is shown in **Figure 5**, the voltage of Pt-Ir/Ti_4O_7 at 1 A/cm^2 only decreased 19 mV, while using Pt/C as the anode catalyst with the loading of Ir is as high as 0.1 mg/cm^2, the voltage decrease is still higher than that of 50 mV. In addition, it is also found that Ir/Ti_4O_7 with low Pt can replace Pt/Ti_4O_7 as an anode catalyst, and Ir/Ti_4O_7 with low Pt has excellent HOR activity and high OER activity. Lee et al. (2020) prepared $IrRu_4/Ti_4O_7$ with 20% mass fraction of IrRu from commercial Ti_4O_7 as an anode catalyst. Compared with 20wt.% commercial Pt/C catalyst, the HOR activity of $IrRu_4/Ti_4O_7$ is similar to that of 20wt.% commercial Pt/C, but the reversal tolerance ability of using $IrRu_4/Ti_4O_7$ is much higher than that of Pt/C. Zhu et al. (2017) synthesized Pt/C by modifying Pt by hydrophobic ionic liquids. The modified Pt/C catalysts showed excellent oxygen reduction and oxygen evolution performance due to its high ionic conductivity and excellent oxygen solubility of protons ionic liquids. The OER performance of the Pt/C catalyst modified by protons ionic liquids is helpful to protect the carbon group from oxidation and obtain a certain antireversal ability. Jung (2011) used carbon nanotube-supported Pt as a cathode catalyst to study the durability of Pt/CNT under anode reversal. Compared with the application of carbon black, CNT has a smaller edge area and less carbon corrosion when the reversal occurs, which is helpful to alleviate the sintering of Pt particles and boost the durability of MEA. The way to boost the durability of MEA is to increase the loading of anode catalyst, cover the surface of anode catalyst support, or use oxidation-resistant catalyst support. Knights et al. (Knights et al., 2003) believed that increasing the catalyst coverage to greater than 9% of support surface area or decreasing the relative interface perimeter of the catalyst and support to less than 4 × 1010 m/g can help improve the voltage reversal tolerance, and the higher the graphitization extent of support is, the better the voltage reversal tolerance will be.

Wang et al. (2020c) synthesized octahedral PtNi/C which has better electrochemical activity and durability than JM Pt/C. The electrochemical activity of PtNi/C decreased slightly when IrO_2, RuO_2, and PtNi/C were mixed as a composite anode and the PtNi/C catalyst was used as a cathode. Compared with only PtNi/C as a cathode and anode catalyst, the electrochemical activity of composite anode remained higher after accelerated durability test. Especially under the condition of continuous reversal test, the durability of MEA prepared by the composite anode was extended by 1 h. Hee-sun Kim et al. (Kim et al., 2021) deposited nano-Ir on the Pt/C catalyst and oxidized it at a high temperature to obtain Pt-IrO_2/C catalyst. The carbon support is multi-defect carbon support, which is traditionally considered to be more prone to carbon corrosion. IrO_2 anchored on the support surface can better protect the support, so that the durability of the fuel cell can be as long as 44 h. Because of the higher specific surface area of multi-defect carbon base, IrO_2 has higher OER activity and

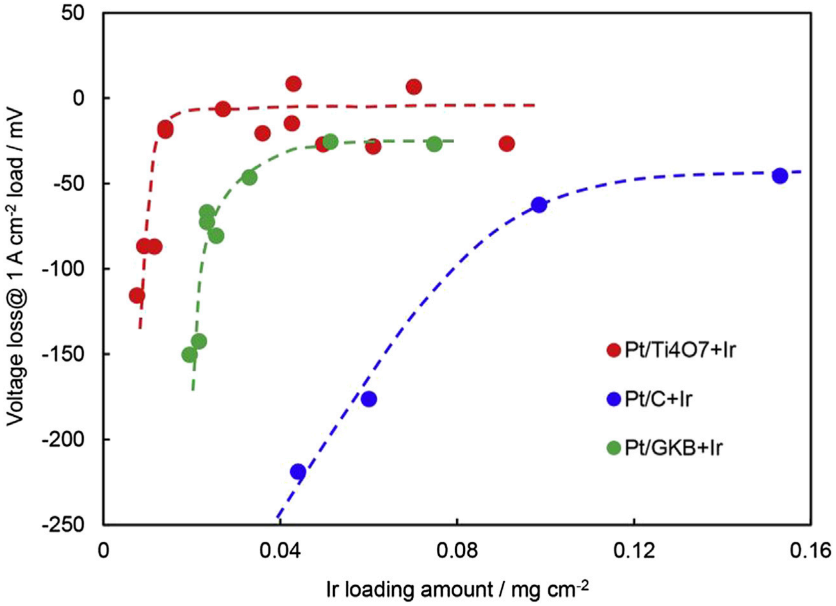

FIGURE 5 | Voltage loss of MEA with various RTAs at 1 A/cm^2 after the reversal test for approximately 2 h (H_2 and O_2 were humidified and the flow is 100 ml/min each, ambient pressure, 80°C). Reproduced with permission (Ioroi and Yasuda, 2020). Copyright 2020, Elsevier.

resistance to CO poisoning. Through the on-line mass spectrometer monitoring, the continuous release of O_2 under the condition of reactant starvation could be observed. When the fuel cell begins to fail, the emission of CO_2 increases continuously. The treatment temperature of the Pt-IrO_2/C catalyst was also studied, and the treatment effects of 250°C, 300°C, 350°C, and 400°C on Pt-IrO_2/C were compared. It is not conducive to the formation of IrO_2 at a low temperature; however, excessive temperature will cause IrO_2 particles to agglomerate and reduce the specific surface area, and the performance of Pt-IrO_2/C synthesized at the treatment temperature of 300°C is the best.

MEA DESIGN APPROACHES

The addition of OER catalyst into the anode has two constraints that need to be considered, one challenge is the stability of OER catalyst in acid media, another challenge is the cost. Controlling the hydrophilicity or hydrophobicity within the catalyst layer, changing the morphology in the catalyst layer, or improving the corrosion resistance of parts had been proved valid to alleviate deterioration from MEA level.

(Mandal et al., 2015) analyzed the change in the Pt/C catalyst after reversal through nano-CT imaging technology and electrochemical diagnosis. The result shows that the reversal results in the collapse of the structure of the anode CL rather than the inter-facial exfoliation between the CL and the PEM. It is generally considered that the performance degradation caused by the reversal is ascribed to the COR of the anode catalyst support. Many previous studies on fuel deficiency have shown that IrO_2, as a RTA catalyst, can inhibit the deterioration of COR of MEA. Hu et al. (2019a) found that when the fuel cell operated below the freezing point, the addition of OER catalyst to the anode had little effect on the reversal tolerance ability. Repeated hydrogen starvation tests were carried out on a single cell at a freezing point temperature of −5°C. It was found that there was no significant change in the polarization curve and EIS curve of the fuel cell. By observing the performance at different temperatures, comparing the performance of fuel cells without IrO_2 catalyst from 15 to 20°C and fuel cells with 5wt% IrO_2 catalyst from 15 to 45°C, they found that carbon corrosion was well suppressed below 0°C. At 10°C and above, the COR of anodes without IrO_2 becomes obvious. Katie Heeyum Lim et al. (Lim et al., 2017) found that the application of graphitized carbon support and OER catalyst in the anode can effectively alleviate the effect of voltage reversal even if 1wt% IrO_2 was added by monitoring the voltage and the concentration of O_2 and CO_2 emissions in the anode side by on-line mass spectrometer. The reversal tolerance time increased significantly and carbon corrosion was inhibited at higher temperature (>40°C) with the addition of IrO_2. The significantly shortened duration of the water electrolysis platform below the freezing point temperature may be attributed to the limited availability of liquid water due to the limitation of the unfrozen proportion of water and its fluidity.

The addition of OER catalyst is an effective way to alleviate the voltage reversal, but the addition of OER catalyst cannot avoid failure. Leining Hu et al. (Hu et al., 2021) found that the performance degradation still occurs when applying Pt black as an anode catalyst, which is speculated to be caused by COR in the microporous layer of the gas diffusion layer (GDL). Based on this conjecture, they utilized Pt black as an anode catalyst, and the coated anode CL with Ti layer with a thickness of 13 um. The results showed that the decay rate of voltage decreased from 15.2%/min to 0.049%/min, and the durability was increased by approximately 310 times. Wang et al. (2020d) studied the influence of gas humidity on reversal tolerance ability, and found that humidity had the opposite effect on reversal tolerance ability when the inlet humidity was greater than 55%. The reversal tolerance failure time of the anode CL area near the inlet is shorter than that near the outlet, and the reversal tolerance ability is better in the MEA region on the side of the air inlet with a higher loading of IrO_2. Joo et al. (2020) Joo suggested that the performance of RTA drops prominently at high humidity because of accelerated poisoning by carbon corrosion species rather than electrical isolation caused by corrosion of carbon support. They found the OER activity of IrO_2 increases linearly with relative humidity, while the rate of COR increases exponentially with relative humidity. Chi-Yeong Ahn et al. (Ahn et al., 2021) investigated the influence of different IrO_2 content in the anode CL on the performance of the MEA and found that the influence was negligible when the IrO_2 content in the anode CL was less than 5%. With further increase in the IrO_2 content in the anode CL, the performance decreased with the increase in ohmic resistance, but the durability increased with the increase in the IrO_2 content. Xiaoyang Zhou et al. (Zhou et al., 2021) designed an RTA, and after the fuel starvation test, the voltage of the MEA attenuates only 0.12% per hour at 1.2 A/cm^2. It is considered that the increase in mass transfer resistance is the primary reason for the increase in anode potential. Moreover, the location of IrO_2RuO_2 has a huge influence on the reversal tolerance ability. Compared with the three ways of blending, IrO_2RuO_2 and Pt/C doping, coating the IrO_2RuO_2 layer first and then coating the Pt/C layer, and coating the Pt/C layer first and then coating the IrO_2RuO_2 layer, the effect of coating 20wt% IrO_2RuO_2 catalyst on the layer of Pt/C is the best, and the durability is as long as 853 min, and with the increase in IrO_2RuO_2 catalyst load, the durability can be as long as 5020 min.

Bentele et al. (2021) reported the normal failure reason is the voltage loss and failure caused by the raising of HOR dynamics and mass transfer resistance, and the increase in mass transport overpotential indicates the collapse of the anode CL caused by COR. In addition, two different HOR catalysts were compared, and it was found that the durability of the RTA was also significantly dependent on the HOR catalyst. Moreover, the OER catalyst is still active after the collapse of the anode CL, and the activity of the surface OER catalyst is not necessarily related to the structural integrity of the anode. Mandal et al. (2018) analyzed the mechanism of antireversal failure by means of electrochemical means and X-ray tomography. The RTA performance improved with the increased loading of IrO_2. However, although IrO_2 was added, RTA failure would still occur. Through the postimaging images, it was found that there was no significant distribution and morphological change of IrO_2 particles in the anode CL. The characteristics and mechanism of failure are similar to those of the MEA without the OER catalyst, which indicates that COR occurs at the same time of water electrolysis, and the collapse of anode CL resulted in the increase in ohmic resistance and the degradation of performance.

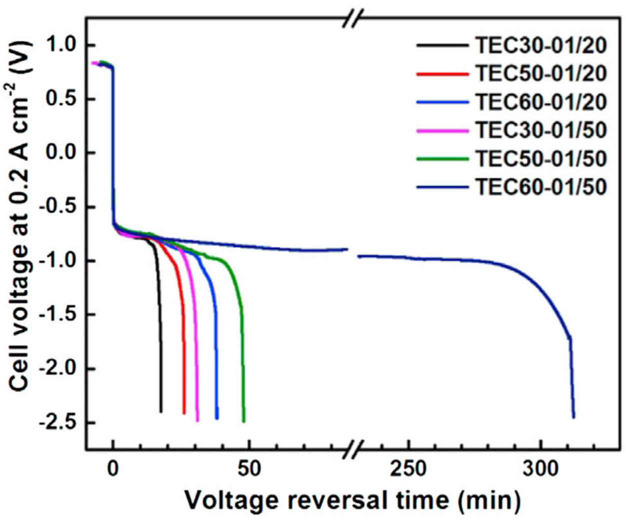

FIGURE 6 | Influence of anode CL thickness and IrO_2 loading on the durability of the RTA. Reproduced with permission (Chen et al., 2021b). Copyright 2021, Elsevier.

(Hong et al., 2016) by means of electrochemical methods and nano-X-ray tomography technology found that the performance of RTA not only attenuates rapidly under the condition of dehydration but also attenuates quantitatively when the humidity increases from 68 to 82%. However, most of the reversal phenomena occur in cold start-up or flooding conditions, which will lead to high humidity conditions. The performance decline of MEA caused by reversal will be accompanied by carbon corrosion, so it can be judged that the final disappearance of OER electrolytic activity is not only the disappearance of IrO_2 itself. This puts forward some opinions on how to solve the potential risk of fuel cells based on materials, and emphasizes the necessity of MEA design, material optimization, and operation strategies to improve RTA performance.

Chen et al. (2021b) compared the influence of the thickness of anode CL on the antireversal time and found that the reversal tolerance ability of the traditional anode CL with only Pt/C is poor and the durability was basically the same regardless of the thickness. As shown in **Figure 6**, for instance, the TEC30-01/20 means the anode CL consists of 0.1 mg/cm^2 of TEC10E30TPM Pt/C and 20 mg/cm^2 of IrO_2. The TEC60-01/50 means the anode CL consists of 0.1 mg/cm^2 of TEC10E50TPM Pt/C and 50 mg/cm^2 of IrO_2. The thinner the anode CL with same loading of IrO_2 is, the better the reversal tolerance ability is. The results show that the durability is as long as 310 min when the thickness of the anode CL is approximately 2 um. It is considered that the effect of thickness on the reversal tolerance ability is mainly due to the distribution of ionomer on the surface of the OER catalyst. In addition, the results showed that the durability prolonged with the increase in loading of IrO_2 and the mass ratio of ionomer to carbon support.

Cai et al. (2020) monitored the change in the electrical resistance of the MEA during the reversal process and found that the electrical resistance of the MEA increased slowly at the

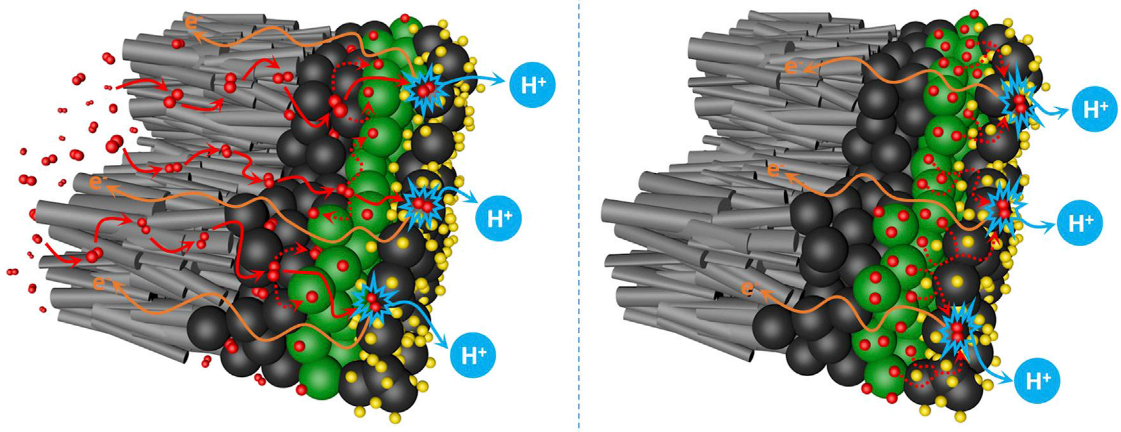

FIGURE 7 | Schematic of TiVCr layer mitigating the reversal.

water electrolysis voltage platform, but increased rapidly after the end of the water electrolysis voltage platform. The correction voltage of electrical resistance shows that the end of the water electrolysis platform is not the deactivation or lack of water of OER catalyst, but the increase in internal resistance caused by carbon corrosion. Yu Zhang et al. (Zhang et al., 2018) investigated the degradation of GDL after the durability test; they found the attenuation of GDL accounted for 13.36% of the whole attenuation of MEA. Yajun Wang et al. (Yajun et al., 2019) designed a test pool in which current density sensors are added to the cathode plate, temperature and humidity sensors are added to the anode plate. It is found that the failure of the RTA is primarily ascribed to the destruction of the electronic path in the GDL, CL, and bipolar plate caused by carbon corrosion instead of the inactivation of the OER catalyst. In addition, In addition, adding OER catalyst to the GDL can significantly improve the reversal tolerance ability of fuel cells. Shengyu Fang et al. (Fang et al., 2014) coated anode GDL with TiVCr hydrogen storage alloy by direct current sputtering, the MEA with TiVCr-coated GDL shows greater durability than MEA with uncoated GDL under no hydrogen condition. As shown in **Figure 7**, the TiVCr layer absorbs hydrogen to saturation and releases hydrogen during starvation, the released hydrogen can mitigate the voltage reversal. Hao et al. (2015) replaced XC-72 with antimony-doped tin oxide as a microporous layer; the GDL with antimony-doped tin oxide MPL shows better durability after oxidation for 55 h.

STACK AND SYSTEM STRATEGIES APPROACHES

The high potential of the anode will accelerate the COR and lead to the degradation of the anode CL in a short period, resulting in the irreversible performance attenuation of MEA (Liu and Hou, 2013; Matsuura et al., 2013; Zhang et al., 2017; Malinowski et al., 2019). Zhong et al. (2018) optimized the flow field design by simulation to improve the distribution of hydrogen in the flow field to obtain uniform and distinct current density. Scott et al. (2015) changed the series structure of the traditional stack by changing the structural design of the stack. The bipolar plate, which is used to distribute reactants, was changed to supply only one kind of reactant, and the MEA was also adjusted from the original cathode face to anode to cathode face to cathode. The stack can still work normally after some cells failed. Cell voltage monitor (CVM) has been used to monitor the voltage of individual cells in stack for the control unit to avoid the occurrence of reversal (Debenjak et al., 2015; Vivas et al., 2019; Shin et al., 2020); the additional accessories involved will not only increase the complexity of the system and reduce the cost efficiency, but also cannot solve the reversal problem. The second solution is the improvement of system hardware materials. But it is expensive and complicated for the fuel cell system. Optimizing the control strategy would be effective to prevent voltage reversal. Control strategies generally monitor operation parameters and feedback by adjusting pressure, flow, and load change, and controlling the stack temperature and gas humidity.

Voltage reversal damage can be minimized by adjusting the stoichiometric ratio of fuel and air, temperature, current load, water management, and other operating parameters. Taniguchi et al. (2008) investigated the effect of reversal caused by air deficiency on the performance of MEA. After the reversal test of 120 min, the size of Pt particles in the cathode CL increased and the electrochemical specific surface area (ECSA) of the cathode CL decreased, which accelerated the performance decay and permanent damage of the MEA while there was no degradation in the anode CL. Taniguchi et al. (2004) studied the influence of hydrogen starvation on the performance of the MEA. The EDX of the anode CL clearly showed that Ru was dissolved from the anode CL and serious Ru loss was found in the hydrogen

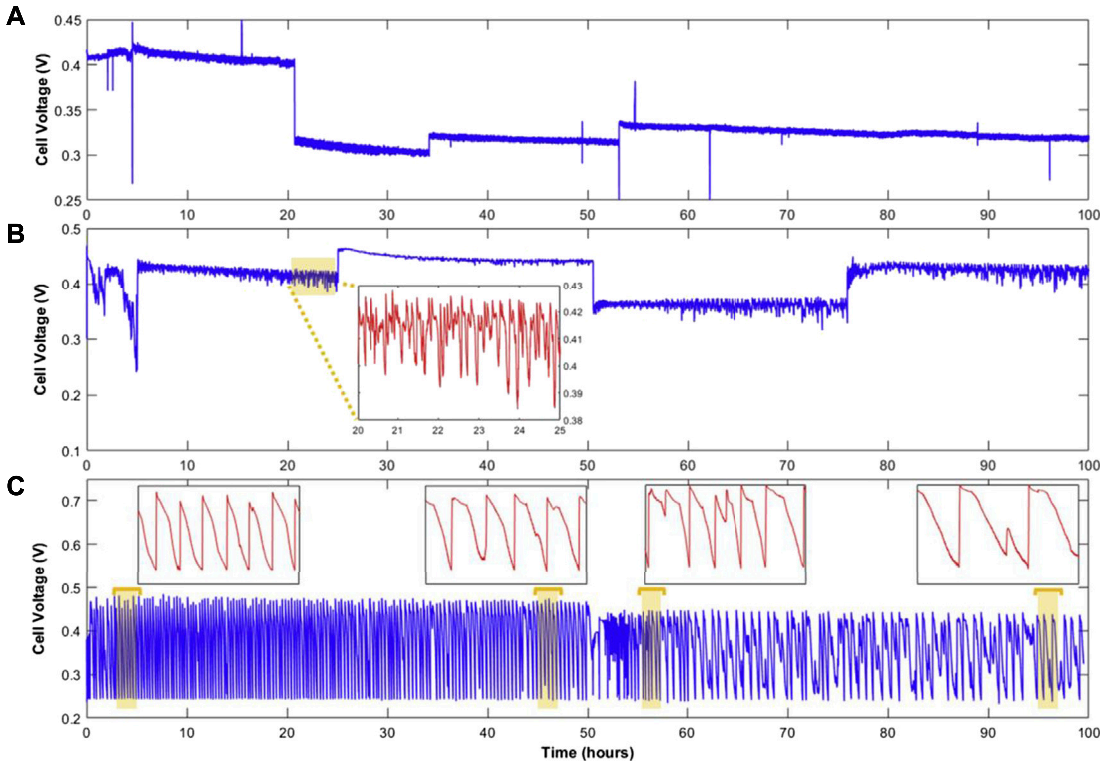

FIGURE 8 | Voltage transient at 0.67 A/cm^2 with 3 modes of operation: flow through **(A)**, anode bleeding, **(B)** dead-end anode **(C)**. In **(B)**, the inset demonstrates the 5-h portion of the specified area. In **(C)**, the 2-h insets show the frequency of the dead-end anode cycles. Reproduced with permission (Eskin and Yesilyurt, 2019). Copyright 2021, Elsevier.

outlet area. Through CO stripping voltammetry and the test of degraded MEA, it was found that the tolerance of MEA to CO decreased. The specific surface area loss of Pt in the cathode CL was found by TEM and CV.

Enhancing the stiochiometric ratio of fuel and air is necessary to avert starvation. Zhou et al. (2015) found that when the stoichiometric ratio of H_2 is less than 1, the voltage of the MEA decreases coupled with the local current density that begins to differ, the current density near the hydrogen inlet shows an upward trend, and the current density near the hydrogen outlet shows a downward trend. When the reversal occurs, CO_2 and O_2 can be detected at the hydrogen outlet. When the load further increases and the stoichiometric ratio decreases, the problem of uneven current density is more serious. Dou et al. (2011) investigated the influence of air starvation by *in situ* monitoring of the local interface potential, current, and temperature distribution of MEA. The results showed that the local potential of the air inlet area remains positive. In contrast, the local potential of the middle and outlet areas becomes negative during the redox reaction, indicating that the reduction reactions can occur in different regions of the cathode at the same time. Before the occurrence of the reversal, with the decrease in the air stoichiometric ratio, the current distribution will be more uneven. When the voltage reversal occurs, the current will be redistributed and will tend to be uniform. At the critical point of voltage reversal, the nonuniformity of current distribution is the most significant. The temperature distribution in the MEA was also monitored online. When the reversal occurred, lots of hot spots were found in the MEA. The study of air stoichiometric ratio at the critical point of voltage reversal under different loads shows that the critical point of air stoichiometric ratio increases with the increase in load. Bing Li et al. (Li and Drew, 2015) found that the rapid change in loading frequency leads to agglomeration of catalyst particles in the anode, which leads to the decline in the performance of MEA, as the rate of mass transfer cannot meet the load demand. Ye Peng et al. (Peng et al., 2021) compared constant current and pulse-accelerated pressure tests to study the RTA ability of MEA. It was found that the pulse test caused more serious MEA damage than the galvanostatic experiment at the same total reversal time. It is possible that each oxidation/reduction cycle accelerates the dissolution of Pt and carbon corrosion. On the contrary, in the galvanostatic test, the COR is relatively slow due to the accumulation of passivation layer or products. The mainway to solve this problem is to optimize system control strategy and stack structure, in which the exhaust composition of anode and cathode outlet, voltage, and local density are monitored by specially designed software (YehLai and Rapaport, 2013; Hu et al., 2019b; Pan et al., 2019; Chen et al., 2020).

Eskin et al. (Eskin and Yesilyurt, 2019) investigated the effect of three different anode exhaust modes on stability and durability.

TABLE 1 | Pros and cons of different approaches for mitigating voltage reversal.

Approach		Pros	Cons
OER catalyst or durable HOR catalysts	IrO_2-Pt/C	Owns HOR and OER activity	Cost increased, HOR activity decreased
	$IrRu_x$/C	Owns HOR and OER activity	Cost increased, HOR activity decreased
	IrO_2/RuO_2	Good reversal tolerance	Cost increased, HOR activity decreased
	Ru_xIr_y	Better than the mixture of Ir and Ru	Cost increased, HOR activity decreased
	$IrRu_4Y_{0.5}$/C	Better HOR than Pt/C and OER activity	High cost
	IrO_x/TiO_2	High durability of support	Less electrical conductivity and lower HOR activity, cannot protect GDL
	Pt/RuO_2-TiO_2	High durability of support	Less electrical conductivity and lower HOR activity, cannot protect GDL
	Ir-Pt/Ti_4O_7	Excellent HOR and OER activity	Cost increased, cannot protect GDL
	$IrRu_4/Ti_4O_7$	High durability of support	Cost increased, less electrical conductivity and lower HOR activity, cannot protect GDL
	Pt/CNT	Improved durability of support	smaller edge area and lower HOR activity, cannot protect GDL
MEA design approaches	Decrease the thickness of the anode CL	Good voltage reversal tolerance and does not increase material cost	Requires high precision coater
	Coating TiVCr hydrogen storage alloy layer on MPL by current sputtering	Can release H_2 under starvation	High cost and complex process, the risk of dissolution
	Addition of OER catalyst in anode	Durability increased with the increase in IrO_2 content	Ohmic resistance increased, cost increased
	Air inlet of MEA with higher loading of IrO_2	Better RTA performance, save material	Complex process and difficult for batch production
	Coating IrO_2RuO_2 catalyst on layer of Pt/C	Better RTA performance	Cost increased
	Replaced XC-72 with antimony-doped tin oxide as microporous layer	Effective to protect MPL from corrosion	Cannot remit the occurrence of voltage reversal and protect the anode CL
Stack and system	Optimize the flow field design	Improve the distribution of fuel, reduce the flooding	Cannot avoid extreme condition
	Changing the structural design of the stack	The stack can still work normally after some cells failed	Increased the complexity of process
	Increase stoichiometric ratio	Better performance, no structure change	Exorbitant stoichiometric ratio would cause power consumption increase, high requirement for air compressor
	Change of loading frequency	No cost from materials, avoids sharp change in current	Cannot avoid extreme condition
	Anode exhaust modes	Alleviate the voltage fluctuation	
	Monitoring cell voltage	Discover the reversal on time	Increased complexity of system and cost

The differential pressure between the anode and the cathode was 1 bar to reduce the penetration of nitrogen into the anode. The change in ECSA of the CL was compared by cyclic voltammetry (CV). As shown in **Figure 8**, compared with the dead-end anode mode and flow through mode, the anode bleeding can effectively alleviate the voltage fluctuation and performance degradation through the syringe pump. With the increase in the pumping speed of the injection pump, the fluctuation of voltage is reduced. Although the operation strategies can effectively prolong the lifetime of the fuel cell, it needs peripheral sensors to monitor and back feed information to adjust the parameters to operate stably. Chen et al. (2016) optimized the opening size of the cathode outlet and found the carbon corrosion of support in both sides becomes less serious with the increase in opening size under the dead-ended anode mode. Lizhong Luo et al. (Luo and Jian, 2019) found that the system strategy can help alleviate the fuel cell reversal phenomenon and boost the performance of the stack. By replacing the single-way solenoid valve used in the closed anode with a three-position three-way solenoid valve, the results show that the maximum power of the air-cooler stack increased by 10.96%, which significantly improves the distribution of hydrogen in the anode channel and reduces the voltage fluctuation. In fact, fuel cell reversal does not take long to occur. Lin et al. (2018) found that the step load strategy is more efficient in mitigating the COR caused by reversal during startup and shutdown operations. (KimHan and Jeong, 2018) Juhan Kim et al. provided the stack with anode reversal tolerance during cold start by measuring the cell voltage, by judging whether the voltage is reversal voltage and comparing the voltage with reference value to judge whether in water electrolysis state, if not, limit the current of stack or shut down, if yes, execute cold start.

The pros and cons of the aforementioned approaches are summed up in **Table 1**.

CONCLUSION

Abnormal operating conditions that cannot provide sufficient H_2 to generate the required electron and proton lead to irreversible damage to the MEA and hence the PEMFC stack as a whole. The degradation factors include carbon corrosion, catalyst sintering and agglomeration, and membrane degradation.

Mitigating reversal can be achieved at three different levels of design: 1) materials, 2) MEA, and 3) system. By optimizing the carbon support and adding OER catalyst into the CL, damage due to reversal can be significantly mitigated. Furthermore, changing the morphology and location of the OER catalyst in the CL and replacing the carbon support with conductive oxides can help increase the anode lifespan. At the MEA level, optimizing the design, such as using more voltage reversal tolerant GDL, or protecting the CL by an inactive metal, is a possible solution to alleviate performance degradation. Finally, the anode can be protected by an appropriate control strategy at the system level. Due to limited supply and rapidly increasing prices of Ir, future efforts will have to focus on developing either non-Ir reversal catalysts or a more advanced system level to eliminate the use of Ir in the MEA altogether.

AUTHOR CONTRIBUTIONS

ZX: conceptualization, investigation, writing—original draft; BW: resources; DB: review and editing; SC: review and editing; ZX: supervision; YL: resources; SL: supervision and review.

ACKNOWLEDGMENTS

The authors acknowledge financial support from the National Key Research and Development Program of China (No. 2018YFB1502502) and the Science and Technology Innovation Program of Hunan Province (2021RC1001).

REFERENCES

Ahn, C.-Y., Kang, S. Y., Choi, H. J., Kim, O.-H., Sung, Y.-E., and Cho, Y.-H. (2021). Effect of Anode Iridium Oxide Content on the Electrochemical Performance and Resistance to Cell Reversal Potential of Polymer Electrolyte Membrane Fuel Cells. *Int. J. Hydrogen Energ.* 4627, 14713–14723. doi:10.1016/j.ijhydene.2021.01.199

Anu, Ksai., and Cindrella, L. (2019). Self-humidifying Novel Chitosan-Geopolymer Hybrid Membrane for Fuel Cell Applications. *Carbohydr. Polym.* 223, 115073. doi:10.1016/j.carbpol.2019.115073

Bentele, D., Aylar, K., Olsen, K., Klemm, E., and Eberhardt, S. H. (2021). PEMFC Anode Durability: Innovative Characterization Methods and Further Insights on OER Based Reversal Tolerance. *J. Electrochem. Soc.* 1682, 024515. doi:10.1149/1945-7111/abe50b

Bhanja, P., Mohanty, B., Patra, A. K., Ghosh, S., Jena, B. K., and Bhaumik, A. (2019). IrO2 and Pt Doped Mesoporous SnO2 Nanospheres as Efficient Electrocatalysts for the Facile OER and HER. *ChemCatChem* 111, 583–592. doi:10.1002/cctc.201801312

Bizon, N., Lopez-Guede, J. M., Kurt, E., Thounthong, P., Mazare, A. G., Ionescu, L. M., et al. (2019). Hydrogen Economy of the Fuel Cell Hybrid Power System Optimized by Air Flow Control to Mitigate the Effect of the Uncertainty about Available Renewable Power and Load Dynamics. *Energ. Convers. Manage.* 179, 152–165. doi:10.1016/j.enconman.2018.10.058

Cai, C., Rao, Y., Zhou, J., Zhang, L., Chen, W., Wan, Z., et al. (2020). Carbon Corrosion: A Novel Termination Mechanism of the Water Electrolysis Plateau during Voltage Reversal. *J. Power Sourc.* 473, 228542. doi:10.1016/j.jpowsour.2020.228542

Chalgin, A. (2020). Effect of Supporting Materials on the Electrocatalytic Activity, Stability and Selectivity of noble Metal-Based Catalysts for Oxygen Reduction and Hydrogen Evolution Reactions. *Prog. Nat. Sci.* 303, 15–23. doi:10.1016/j.pnsc.2020.01.003

Chen, B., Wang, J., Yang, T., Cai, Y., Pan, M., Tu, Z., et al. (2016). Mitigation Studies of Carbon Corrosion by Optimizing the Opening Size of the Cathode Outlet in a Proton Exchange Membrane Fuel Cell with Dead-Ended Anode. *Energ. Convers. Manage.* 119, 60–66. doi:10.1016/j.enconman.2016.04.043

Chen, K., Laghrouche, S., and Djerdir, A. (2019). Degradation Prediction of Proton Exchange Membrane Fuel Cell Based on Grey Neural Network Model and Particle Swarm Optimization. *Energ. Convers. Manage.* 195, 810–818. doi:10.1016/j.enconman.2019.05.045

Chen, K., Laghrouche, S., and Djerdir, A. (2021). Performance Analysis of PEM Fuel Cell in mobile Application under Real Traffic and Environmental Conditions - ScienceDirect. *Energ. Convers. Manage.* 227, 1136002. doi:10.1016/j.enconman.2020.113602

Chen, W., Cai, C., Li, S., Tan, J., and Pan, M. (2021). Thickness Effects of Anode Catalyst Layer on Reversal Tolerant Performance in Proton Exchange Membrane Fuel Cell. *Int. J. Hydrogen Energ.* 4612, 8749–8757. doi:10.1016/j.ijhydene.2020.12.041

Chen, X., Xu, J., Liu, Q., Chen, Y., Wang, X., Li, W., et al. (2020). Active Disturbance Rejection Control Strategy Applied to Cathode Humidity Control in PEMFC System. *Energ. Convers. Manage.* 224, 113389. doi:10.1016/j.enconman.2020.113389

Cheng, W. (2015). The Durability Research on the Proton Exchange Membrane Fuel Cell for Automobile Application. *Prog. Chem.* 274, 424–435. doi:10.7536/PC140807

Cullen, D. A., More, K. L., Atanasoska, L. L., and Atanasoski, R. T. (2014). Impact of IrRu Oxygen Evolution Reaction Catalysts on Pt Nanostructured Thin Films under Start-Up/shutdown Cycling. *J. Power Sourc.* 269, 671–681. doi:10.1016/j.jpowsour.2014.06.153

Jung, D.-W. (2011). Durability of Polymer Electrolyte Membrane Fuel Cell with Pt/CNTs Catalysts in Cell Reversal Conditions by Hydrogen Starvation. *Fuel Cells* 116, 866–874. doi:10.1002/fuce.201100034

Dang, D., Zhang, L., Zeng, X., Tian, X., Qu, C., Nan, H., et al. (2017). *In Situ* construction of Ir@Pt/C Nanoparticles in the Cathode Layer of Membrane Electrode Assemblies with Ultra-low Pt Loading and High Pt Exposure. *J. Power Sourc.* 355, 83–89. doi:10.1016/j.jpowsour.2017.04.050

Debenjak, A., Petrovcic, J., Boskoski, P., Musizza, B., and Juricic, D. (2015). Fuel Cell Condition Monitoring System Based on Interconnected DC-DC Converter and Voltage Monitor. *IEEE Trans. Ind. Electron.* 628, 5293–5305. doi:10.1109/tie.2015.2434792

Dhanushkodi, S. R., Tam, M., Kundu, S., Fowler, M. W., and Pritzker, M. D. (2013). Carbon Corrosion Fingerprint Development and De-convolution of Performance Loss According to Degradation Mechanism in PEM Fuel Cells. *J. Power Sourc.* 24015 (oct), 114–121. doi:10.1016/j.jpowsour.2013.03.033

Dong, L. (2009). Study of the Cell Reversal Process of Large Area Proton Exchange Membrane Fuel Cells under Fuel Starvation. *J. Power Sourc.* 1942, 847–853. doi:10.1016/j.jpowsour.2009.06.059

Dou, M., Ming, H., and Dong, L. (2011). Behaviors of Protons Exchange Membrane Fuel Cells under Oxidant Starvation. *J. Power Sourc.* 5, 2759–2762. doi:10.1016/j.jpowsour.2010.11.005

Dustin, B., Ja-Yeon, C., Takeaki, K., and Siyu, Y. (2019). Integrating PGM-free Catalysts into Catalyst Layers and Proton Exchange Membrane Fuel Cell Devices. *Adv. Mater.* 3131, 1804846. doi:10.1002/adma.201804846

Eskin, M. G., and Yesilyurt, S. (2019). Anode Bleeding Experiments to Improve the Performance and Durability of Protons Exchange Membrane Fuel Cells. *Int. J. Hydrogen Energ.* 44, 2111047–2111056. doi:10.1016/j.ijhydene.2019.02.152

Fan, L., Zhang, G., and Jiao, K. (2017). Characteristics of PEMFC Operating at High Current Density with Low External Humidification. *Energ. Convers. Manage.* 150, 763–774. doi:10.1016/j.enconman.2017.08.034

Fang, S.-Y., Huang, R.-H., Teoh, L. G., Hsueh, K.-L., Chao, W.-K., Tsai, D.-C., et al. (2014). Coating TiVCr Hydrogen Storage alloy on the Anode Gas Diffusion Layer of Proton Exchange Membrane Fuel Cells to Improve Performance. *J. Power Sourc.* 268, 443–450. doi:10.1016/j.jpowsour.2014.06.072

Hao, J., Yu, S., Jiang, Y., Li, X., Shao, Z., and Yi, B. (2015). Antimony Doped Tin Oxide Applied in the Gas Diffusion Layer for Proton Exchange Membrane Fuel

Cells. *J. electroanalytical Chem.* 7561, 201–206. doi:10.1016/j.jelechem.2015.08.035

Hasché, F., Oezaslan, M., and Strasser, P. (2010). Activity, Stability and Degradation of Multi Walled Carbon Nanotube (MWCNT) Supported Pt Fuel Cell Electrocatalysts. *Phys. Chem. Chem. Phys.* 1246, 15251–15258. doi:10.1039/c0cp00609b

Hong, B. K., Mandal, P., Oh, J.-G., and Litster, S. (2016). On the Impact of Water Activity on Reversal Tolerant Fuel Cell Anode Performance and Durability. *J. Power Sourc.* 328, 280–288. doi:10.1016/j.jpowsour.2016.07.002

Hou, S. (2019). Enhanced Low-Humidity Performance in a Proton Exchange Membrane Fuel Cell by Developing a Novel Hydrophilic Gas Diffusion Layer. *Int. J. Hydrogen Energ.* 451, 937–944. doi:10.1016/j.ijhydene.2019.10.160

Hu, L., Hong, B. K., Oh, J.-G., and Litster, S. (2021). Reversal Tolerant Anodes Using Protective Layers for Highly Robust Automotive Fuel Cells. *ACS Appl. Energ. Mater.* 41, 119–127. doi:10.1021/acsaem.0c02011

Hu, L., Hong, B. K., Oh, J.-G., and Litster, S. (2019). Robust Operation of Fuel Cell Systems in Subfreezing Conditions: A Material-Based Solution to Achieve Better Anode Durability. *ACS Appl. Energ. Mater.* 210, 7152–7161. doi:10.1021/acsaem.9b01108

Hu, Z. (2021). Mechanistic Insight into the Accelerated Decay of Fuel Cells from Catalyst-Layer Structural Failure. *Energ. Convers. Manage.* 227, 113568. doi:10.1016/j.enconman.2020.113568

Hu, Z., Xu, L., Li, J., Gan, Q., Xu, X., Song, Z., et al. (2019). A Novel Diagnostic Methodology for Fuel Cell Stack Health: Performance, Consistency and Uniformity. *Energ. Convers. Manage.* 185, 611–621. doi:10.1016/j.enconman.2019.02.031

Hu, Z., Xu, L., Li, J., Hu, J., Xu, X., Du, X., et al. (2018). A Cell Interaction Phenomenon in a Multi-Cell Stack under One Cell Suffering Fuel Starvation. *Energ. Convers. Manage.* 174, 465–474. doi:10.1016/j.enconman.2018.08.062

Huang, Z., Shen, J., Chan, S. H., and Tu, Z. (2020). Transient Response of Performance in a Proton Exchange Membrane Fuel Cell under Dynamic Loading. *Energ. Convers. Manage.* 226, 113492. doi:10.1016/j.enconman.2020.113492

Ioroi, T., and Yasuda, K. (2020). Highly Reversal-Tolerant Anodes Using Ti4O7-Supported Platinum with a Very Small Amount of Water-Splitting Catalyst. *J. Power Sourc.* 450, 227656. doi:10.1016/j.jpowsour.2019.227656

Jia, F., Guo, L., and Liu, H. (2017). Mitigation Strategies for Hydrogen Starvation under Dynamic Loading in Proton Exchange Membrane Fuel Cells. *Energ. Convers. Manage.* 139, 175–181. doi:10.1016/j.enconman.2017.02.051

Jia, F., Liu, F., Guo, L., and Liu, H. (2016). Mechanisms of Reverse Current and Mitigation Strategies in Proton Exchange Membrane Fuel Cells during Startups. *Int. J. Hydrogen Energ.* 4115, 6469–6475. doi:10.1016/j.ijhydene.2016.03.037

Jia, Q., Caldwell, K., Strickland, K., Ziegelbauer, J. M., Liu, Z., Yu, Z., et al. (2015). Improved Oxygen Reduction Activity and Durability of Dealloyed PtCox Catalysts for Proton Exchange Membrane Fuel Cells: Strain, Ligand, and Particle Size Effects. *ACS Catal.* 51, 176–186. doi:10.1021/cs501537n

Joo, T., Hu, L., Hong, B. K., Oh, J.-G., and Litster, S. (2020). On the Origin of Deactivation of Reversal-Tolerant Fuel Cell Anodes under Voltage Reversal Conditions. *J. Power Sourc.* 472, 228439. doi:10.1016/j.jpowsour.2020.228439

Kim, H.-E., Shin, S., and Lee, H. (2021). Pt-IrOx Catalysts Immobilized on Defective Carbon for Efficient Reversal Tolerant Anode in Proton Exchange Membrane Fuel Cells. *J. Catal.* 395, 404–411. doi:10.1016/j.jcat.2021.01.028

Kim, T.-Y., Lee, S. W., and Pak, C. (2020). Optimization of Carbon-Supported Ir-Ru Alloys for Polymer Electrolyte Fuel Cell Anodes under Cell Reversal. *J. Ind. Eng. Chem.* 85, 87–93. doi:10.1016/j.jiec.2020.01.024

KimHan, J. W. S. B., and Jeong, K. S. (2018). *Method of Controlling Operation of Fuel Cell.* US Patent. 20180351185A1. (Accessed May 30, 2017).

Knights, S. D., Taylor, J. L., and Wilkinson, D. P. (2003). *Supported Catalysts for the Anode of a Voltage Reversal Tolerant Fuel Cell.* US20040157110A1: WO.

Kumar, A., Atienza, D., and Ramani, V. (2017). "Pt/RuO_2-TiO_2 (RTO) as Cell Reversal Tolerant Anode Catalyst for PEFCs," in *231st ECS Meeting* (New Orleans, LA.

Labi, T. (2021). Increasing Fuel Cell Durability during Prolonged and Intermittent Fuel Starvation Using Supported IrOx. *J. Power Sourc.* 490, 229568. doi:10.1016/j.jpowsour.2021.229568

Lee, S. W., Lee, B., Baik, C., Kim, T.-Y., and Pak, C. (2021). Multifunctional Ir-Ru alloy Catalysts for Reversal-Tolerant Anodes of Polymer Electrolyte Membrane Fuel Cells. *J. Mater. Sci. Techn.* 60, 105–112. doi:10.1016/j.jmst.2020.05.020

Lee, S. W., Lee, B. H., Baik, C., You, E., You, D. J., and Pak, C. (2020). MagnéLi-Phase Ti4O7-Supported Irru-Based Catalysts for Reversal Tolerant Anode of Automotive Polymer Electrolyte Membrane Fuel Cell. *Meet. Abstr.* 0138, 1656. doi:10.1149/ma2020-01381656mtgabs

Lee, S. W., Lee, B. H., Kim, T.-Y., Baik, C., Kim, M. S., Chai, G. S., et al. (2019). Multifunctional Non-pt Ternary Catalyst for the Hydrogen Oxidation and Oxygen Evolution Reactions in Reversal-Tolerant Anode. *Catal. Commun.* 130, 105758. doi:10.1016/j.catcom.2019.105758

Lee, W. H., Ko, Y. J., Kim, J. H., Choi, C. H., Chae, K. H., Kim, H., et al. (2021). High Crystallinity Design of Ir-Based Catalysts Drives Catalytic Reversibility for Water Electrolysis and Fuel Cells. *Nat. Commun.* 12 (2021), 4271. doi:10.1038/s41467-021-24578-8

Li, Bing., and Drew, C. (2015). The Durability of Carbon Supported Pt Nanowire as Novel Cathode Catalyst for a 1.5 kW PEMFC Stack. *Appl. Catal. B: Environ.* 162, 133–140. doi:10.1016/j.apcatb.2014.06.040

Lile, Jrd. (2021). First Principles Study of Ir3Ru, IrRu and IrRu3catalysts for Hydrogen Oxidation Reaction: Effect of Surface Modification and Ruthenium Content. *Appl. Surf. Sci.* 545, 149002. doi:10.1016/j.apsusc.2021.149002

Lim, K. H., Lee, W. H., Jeong, Y., and Kim, H. (2017). Analysis of Carbon Corrosion in Anode under Fuel Starvation Using On-Line Mass Spectrometry in Polymer Electrolyte Membrane Fuel Cells. *J. Electrochem. Soc.* 16414, F1580–F1586. doi:10.1149/2.0731714jes

Lin, R., Xia, S., Zhang, Q., and Dutruel, B. (2018). Comparison between the Constant Dummy Load and Step Load Shut-Down Strategy for PEMFCs. *Fuel Cells* 183, 306–314. doi:10.1002/fuce.201700095

Liu, B., Wang, S., Wang, C.-y., Ma, B.-z., and Chen, Y.-q. (2020). Electrochemical Behavior and Corrosion Resistance of IrO2-ZrO2 Binary Oxide Coatings for Promoting Oxygen Evolution in Sulfuric Acid Solution. *Int. J. Miner Metall. Mater.* 272, 264–273. doi:10.1007/s12613-019-1847-0

Liu, F., Peng, H., Qiao, X., Fu, Z., Huang, P., and Liao, S. (2014). High-performance Doped Carbon Electrocatalyst Derived from Soybean Biomass and Promoted by Zinc Chloride. *Int. J. Hydrogen Energ.* 3919, 10128–10134. doi:10.1016/j.ijhydene.2014.04.176

Liu, G., Xu, J., Wang, Y., Jiang, J., and Wang, X. (2014). A Novel Catalyst Coated Membrane Embedded with Cs-Substituted Phosphotungstates for Proton Exchange Membrane Water Electrolysis. *Int. J. Hydrogen Energ.* 3927, 14531–14539. doi:10.1016/j.ijhydene.2014.07.106

Liu, J., and Hou, Z. (2013). *Carbon Corrosion in Polymer Electrolyte Membrane Fuel Cell Catalysts and its Mitigation Strategies*. Springer Berlin Heidelberg. doi:10.1007/978-3-642-33497-9_3

Luo, L., and Jian, Q. (2019). Experimental Study and Mitigation of Abnormal Behavior of Cell Voltage in a Protons Exchange Membrane Fuel Cell Stack. *Int. J. Energ. Res.* 43 (5), 1912–1923. doi:10.1002/er.4413

Malinowski, M., Iwan, A., Hreniak, A., and Tazbir, I. (2019). An Anode Catalyst Support for Polymer Electrolyte Membrane Fuel Cells: Application of Organically Modified Titanium and Silicon Dioxide. *RSC Adv.* 942, 24428–24439. doi:10.1039/c9ra04862f

Mandal, P., Hong, B. K., Oh, J.-G., and Litster, S. (2015). 3D Imaging of Fuel Cell Electrode Structure Degraded under Cell Voltage Reversal Conditions Using Nanoscale X-Ray Computed Tomography. *ECS Trans.* 6917, 443–453. doi:10.1149/06917.0443ecst

Mandal, P., Hong, B. K., Oh, J.-G., and Litster, S. (2018). Understanding the Voltage Reversal Behavior of Automotive Fuel Cells. *J. Power Sourc.* 397, 397–404. doi:10.1016/j.jpowsour.2018.06.083

Matsuura, T., Chen, J., Siegel, J. B., and Stefanopoulou, A. G. (2013). Degradation Phenomena in PEM Fuel Cell with Dead-Ended Anode. *Int. J. Hydrogen Energ.* 3826, 11346–11356. doi:10.1016/j.ijhydene.2013.06.096

Min, Y., Yuchan, Z., Li, D., Ruoxi, M., and Ailian, Z. (2017). IrO_2-TiO_2 Electrocatalysts for the Hydrogen Evolution Reaction in Acidic Water Electrolysis without Activation. *New J. Chem.* 4114, 6152–6159. doi:10.1039/c7nj00756f

Moore, C. E., Eastcott, J., Cimenti, M., Kremliakova, N., and Gyenge, E. L. (2019). Novel Methodology for *Ex Situ* Characterization of Iridium Oxide Catalysts in Voltage Reversal Tolerant Proton Exchange Membrane Fuel Cell Anodes. *J. Power Sourc.* 417, 53–60. doi:10.1016/j.jpowsour.2019.02.006

Nakashima, N. (2019). Nanocarbons for Energy Conversion: Supramolecular Approaches. *Recent Prog. Non-precious Metal Fuel Cel Catalysts* 11, 253–276. doi:10.1007/978-3-319-92917-0

Pan, T., Shen, J., Sun, L., and Lee, K. Y. (2019). Thermodynamic Modelling and Intelligent Control of Fuel Cell Anode Purge. *Appl. Therm. Eng.* 154, 196–207. doi:10.1016/j.applthermaleng.2019.03.009

Pandy, A., Yang, Z., Gummalla, M., Atrazhev, V. V., Kuzminyh, N. Y., Sultanov, V. I., et al. (2013). A Carbon Corrosion Model to Evaluate the Effect of Steady State and Transient Operation of a Polymer Electrolyte Membrane Fuel Cell. *J. Electrochem. Soc.* 1609, F972–F979. doi:10.1149/2.036309jes

Paul, S., Yong, C., and Rajnish, K. C. (2015). The Effect of Low Platinum Loading on the Efficiency of PEMFC's Electrocatalysts Supported on TiO2–Nb, and SnO2–Nb: An Experimental Comparison between Active and Stable Conditions. *Energ. Convers. Manage.* 103, 681–690. doi:10.1016/j.enconman.2015.06.050

Peng, H., Liu, F., Qiao, X., Xiong, Z., Li, X., Shu, T., et al. (2015). Nitrogen and Fluorine Co-doped Carbon Catalyst with High Oxygen Reduction Performance, Prepared by Pyrolyzing a Mixture of Melamine and PTFE. *Electrochimica Acta* 182, 963–970. doi:10.1016/j.electacta.2015.10.012

Peng, H., Mo, Z., Liao, S., Liang, H., Yang, L., Luo, F., et al. (2013). High Performance Fe- and N- Doped Carbon Catalyst with Graphene Structure for Oxygen Reduction. *Sci. Rep.* 3, 1765. doi:10.1038/srep01765

Peng, Y., Choi, J.-Y., Bai, K., Zhang, Y., and Banham, D. (2021). Pulsed vs. Galvanostatic Accelerated Stress Test Protocols: Comparing Predictions for Anode Reversal Tolerance in Proton Exchange Membrane Fuel Cells. *J. Power Sourc.* 500, 229986. doi:10.1016/j.jpowsour.2021.229986

Petch, M., Burton, S., Hodgkinson, A., O'Malley, R., and Turner, W. (2015). Mitigation of Fuel Cell Degradation through MEA Design. *SAE Int. J. Passeng. Cars - Mech. Syst.* 91, 1–5. doi:10.4271/2015-01-1777

Puthiyapura, V. K., Pasupathi, S., and Su, H. (2014). Investigation of Supported IrO2 as Electrocatalyst for the Oxygen Evolution Reaction in Proton Exchange Membrane Water Electrolyser. *Int. J. Hydrogen Energ.* 39, 51905–51913. doi:10.1016/j.ijhydene.2013.11.056

Roh, C.-W., Kim, H.-E., Choi, J., Lim, J., and Lee, H. (2019). Monodisperse IrOx Deposited on Pt/C for Reversal Tolerant Anode in Proton Exchange Membrane Fuel Cell. *J. Power Sourc.* 443, 227270. doi:10.1016/j.jpowsour.2019.227270

Rui, L. A. (2021). Investigation of Real-Time Changes and Recovery of Proton Exchange Membrane Fuel Cell in Voltage Reversal - ScienceDirect. *Energ. Convers. Manage.* 236, 114037. doi:10.1016/j.enconman.2021.114037

Scott, P., Chen, Y., Calay, R., and Bhinder, F. (2015). Experimental Investigation into a Novel Modular PEMFC Fuel Cell Stack. *Fuel Cells* 152, 306–321. doi:10.1002/fuce.201200212

Shen, J. (2020). Partial Flooding and its Effect on the Performance of a Proton Exchange Membrane Fuel Cell. *Energ. Convers. Manage.* 207, 1125371–1125378. doi:10.1016/j.enconman.2020.112537

Shin, D., Yoo, S., and Lee, Y.-H. (2020). On-line Water Contents Diagnosis of PEMFC Based on Measurements. *Int. J. Precis. Eng. Manuf.-Green Tech.* 76, 1085–1093. doi:10.1007/s40684-020-00232-4

Shin, S. (2020). Numerical Analysis on Transport Properties of Self-Humidifying Dual Catalyst Layer via 3-D Reconstruction Technique. *Int. J. Hydrogen Energ.* 4627, 14639–14650. doi:10.1016/j.ijhydene.2020.07.254

Sibul, R., Kibena-Põldsepp, E., Ratso, S., Kook, M., Sougrati, M. T., Käärik, M., et al. (2020). Iron- and Nitrogen-Doped Graphene-Based Catalysts for Fuel Cell Applications. *ChemElectroChem* 7, 1739–1747. doi:10.1002/celc.202000011

Taniguchi, A., Akita, T., Yasuda, K., and Miyazaki, Y. (2008). Analysis of Degradation in PEMFC Caused by Cell Reversal during Air Starvation. *Int. J. Hydrogen Energ.* 339, 2323–2329. doi:10.1016/j.ijhydene.2008.02.049

Taniguchi, A., Akita, T., Yasuda, K., and Miyazaki, Y. (2004). Analysis of Electrocatalyst Degradation in PEMFC Caused by Cell Reversal during Fuel Starvation. *J. Power Sourc.* 130, 42–49. doi:10.1016/j.jpowsour.2003.12.035

Tovini, M. F., Damjanovi, A. M., and El-Sayed, H. A. (2020). Degradation Mechanism of an IrO2 Anode Co-catalyst for Cell Voltage Reversal Mitigation under Transient Operation Conditions of a PEM Fuel Cell. *J. Electrochem. Socitety* 168, 064521. doi:10.1149/1945-7111/ac0d39

Velikokhatnyi, O. I., Kadakia, K., Datta, M. K., and Kumta, P. N. (2013). Fluorine-Doped IrO2: A Potential Electrocatalyst for Water Electrolysis. *J. Phys. Chem. C* 11740, 20542–20547. doi:10.1021/jp308947h

Vichard, L., Petrone, R., Harel, F., Ravey, A., Venet, P., and Hissel, D. (2020). Long Term Durability Test of Open-Cathode Fuel Cell System under Actual Operating Conditions. *Energ. Convers. Manage.* 212, 112813. doi:10.1016/j.enconman.2020.112813

Vivas, F. J., Heras, A. d. l., Segura, F., and Andújar, J. M., (2019). Cell Voltage Monitoring All-In-One. A New Low Cost Solution to Perform Degradation Analysis on Air-Cooled Polymer Electrolyte Fuel Cells. *Int. J. Hydrogen Energ.* 4425, 12842–12856. doi:10.1016/j.ijhydene.2018.12.172

Wang, H., Gao, Q., Sun, S., Zhang, W., and Yao, S. (2020). CoP@NRGO Composite as a High-Efficiency Water Electrolysis Catalyst for Hydrogen Generation. *J. Solid State. Chem.* 290, 121596. doi:10.1016/j.jssc.2020.121596

Wang, J., Zhou, X., Li, B., Yang, D., Lv, H., Xiao, Q., et al. (2020). Highly Efficient, Cell Reversal Resistant PEMFC Based on PtNi/C Octahedral and OER Composite Catalyst. *Int. J. Hydrogen Energ.* 4515, 8930–8940. doi:10.1016/j.ijhydene.2020.01.054

Wang, T., Wu, H., Feng, C., Zhang, L., and Zhang, J. (2020). MoP@NiCo-LDH on Nickel Foam as Bifunctional Electrocatalyst for High Efficiency Water and Urea-Water Electrolysis. *J. Mater. Chem. A.* 835, 18106–18116. doi:10.1039/d0ta06030e

Wang, Y., Xie, X., Zhou, C., Feng, Q., Zhou, Y., Yuan, X.-Z., et al. (2020). Study of Relative Humidity on Durability of the Reversal Tolerant Proton Exchange Membrane Fuel Cell Anode Using a Segmented Cell. *J. Power Sourc.* 449, 227542. doi:10.1016/j.jpowsour.2019.227542

Wh, A. (2021). Performance Prediction of Proton-Exchange Membrane Fuel Cell Based on Convolutional Neural Network and Random forest Feature Selection. *Energ. Convers. Manage.* 2432, 114367. doi:10.1016/j.enconman.2021.114367

Xiong, Z. a., Liao, S., Dang, D., Tian, X., Hou, S., Liu, F., et al. (2015). Enhanced Water Management in the Cathode of an Air-Breathing PEMFC Using a Dual Catalyst Layer and Optimizing the Gas Diffusion and Microporous Layers. *Int. J. Hydrogen Energ.* 4010, 3961–3967. doi:10.1016/j.ijhydene.2015.01.091

Yajun, W., Chang, Z., and Xiaojun, X. (2019). Study of Failure Mechanisms of the Reversal Tolerant Fuel Cell Anode via Novel *In-Situ* Measurements. *Int. J. Hydrogen Energ.* 451, 996–1007. doi:10.1016/j.ijhydene.2019.10.189

Yanzhou, Q., Du, Q., Mingzhe, F., Yafei, C., and Yan, Y. (2017). Study on the Operating Pressure Effect on the Performance of a Proton Exchange Membrane Fuel Cell Power System. *Energ. Convers. Manage.* 142, 357–365. doi:10.1016/j.enconman.2017.03.035

YehLai, H., and Rapaport, P. A. N (2013). *Stack Operation Method Aimed at Cell Reversal Prevention*. US patent, 8524408B2. (September 25, 2009).

Yi, Y. (2012). A Review on Performance Degradation of Proton Exchange Membrane Fuel Cells during Startup and Shutdown Processes: Causes, Consequences, and Mitigation Strategies. *J. Power Sourc.* 2052, 10–23. doi:10.1016/j.jpowsour.2012.01.059

You, C., Liao, S., Li, H., Hou, S., Peng, H., Zeng, X., et al. (2014). Uniform Nitrogen and Sulfur Co-doped Carbon Nanospheres as Catalysts for the Oxygen Reduction Reaction. *Carbon* 69, 294–301. doi:10.1016/j.carbon.2013.12.028

You, E., Lee, S. W., You, D., Lee, B., and Pak, C. (2020). Effect of Metal Composition and Carbon Support on the Durability of the Reversal-Tolerant Anode with IrRu Alloy Catalyst. *Catalysts* 108, 932. doi:10.3390/catal10080932

Zhang, G., Shen, S., Guo, L., and Liu, H. (2012). Dynamic Characteristics of Local Current Densities and Temperatures in Proton Exchange Membrane Fuel Cells during Reactant Starvations. *Int. J. Hydrogen Energ.* 37 (2), 1884–1892. doi:10.1016/j.ijhydene.2011.04.120

Zhang, X., Yang, Y., Guo, L., and Liu, H. (2017). Effects of Carbon Corrosion on Mass Transfer Losses in Proton Exchange Membrane Fuel Cells. *Int. J. Hydrogen Energ.* 427, 4699–4705. doi:10.1016/j.ijhydene.2016.08.223

Zhang, Y., Tan, J. T., and Pan, M. (2018). *Study on Durability of Gas Diffusion Layers in the Proton Exchange Membrane Fuel Cells. Dissertation for the Master's Degree*. Wuhan: Wuhan University of Technology.

Zhao, N. (2020). Effects of Fuel Cell Operating Conditions on Proton Exchange Membrane Durability at Open-Circuit Voltage. *Fuel Cells* 2, 176–184. doi:10.1002/fuce.201900173

Zhong, D., Lin, R., Liu, D., and Cai, X. (2018). Structure Optimization of Anode Parallel Flow Field for Local Starvation of Proton Exchange Membrane Fuel Cell. *J. Power Sourc.* 403, 1–10. doi:10.1016/j.jpowsour.2018.09.067

Zhou, F., Andreasen, S. J., and Kær, S. K. (2015). Experimental Study of Cell Reversal of a High Temperature Polymer Electrolyte Membrane Fuel Cell Caused by H2 Starvation. *Int. J. Hydrogen Energ.* 4020, 6672–6680. doi:10.1016/j.ijhydene.2015.03.148

Zhou, X., Ji, H., Li, B., and Zhang, C. (2020). High-Repetitive Reversal Tolerant Performance of Proton-Exchange Membrane Fuel Cell by Designing a Suitable Anode. *ACS Omega* 5, 10099–10105. doi:10.1021/acsomega.0c00638

Zhou, X., Yang, Y., Li, B., and Zhang, C. (2021). Advanced Reversal Tolerant Anode in Proton Exchange Membrane Fuel Cells: Study on the Attenuation Mechanism during Fuel Starvation. *ACS Appl. Mater. Inter.* 132, 2455–2461. doi:10.1021/acsami.0c16541

Zhu, Z., Yan, X., Tang, H., Cai, H., Pan, M., Zhang, H., et al. (2017). Protic Ionic Liquid Modified Electrocatalyst Enables Robust Anode under Cell Reversal Condition. *J. Power Sourc.* 351, 138–144. doi:10.1016/j.jpowsour.2017.03.076

Conflict of Interest: The authors declare that the research was conducted in the absence of any commercial or financial relationships that could be construed as a potential conflict of interest.